1

An Introduction to Modulations and Waveforms for 5G Networks

Stefano Buzzi, Alessandro Ugolini, Alessio Zappone and Giulio Colavolpe

1.1 Motivation and Background

Historically, the evolution of wireless cellular systems has been fueled by the need for increased throughput. Indeed, the need for larger data-rates has been the main driver of the path that has led us from 2G systems[1] to 4G systems, with data-rates evolving from tens of kbit/s up to the current state-of-the-art tens of Mbit/s. Focusing on the physical (PHY) layer, and in particular on the adopted modulation schemes, the transition has been from

[1] Indeed analog 1G cellular systems had no data transmission capability; they just offered voice services.

Signal Processing for 5G: Algorithms and Implementations, First Edition. Edited by Fa-Long Luo and Charlie Zhang.

binary modulations such as the Gaussian minimum shift keying (GMSK), used in the 2G GSM system, to quadrature-amplitude-modulation (QAM) schemes with adaptively chosen cardinality, currently used in 4G systems.

Unlike previous generations of cellular networks, 5G systems will have to accommodate a variety of services and of emerging new applications, and, in order to do that, focusing only on the increase of the data throughput is not enough. In particular, according to the classification in Michailow *et al.* [1], the main reference scenarios currently envisioned for 5G networks are as follows.

- **Very large data-rate wireless connectivity**. Users will be able to download large amounts of data in a short time; a typical application corresponding to this scenario is high-definition video streaming, which of course requires a modulation scheme with large spectral and energy efficiency.
- **Internet of Things (IoT)**. Up to one trillion devices are expected to be connected through the 5G network, enabling users to remotely control things such as cars, washing machines, air conditioners, lights, and so on. Likewise, energy, water and gas distribution companies will take advantage of connected smart meters in order to control their networks. These connected things will have quite limited processing capabilities and will have to transmit small amounts of data sporadically, thus requiring a modulation scheme robust to time synchronization errors and performing well for short communications.
- **Tactile Internet** [2]. This scenario refers to real-time cyber-physical tactile control experiments (such as remote control of drones and/or of rescue robots in emergency situations), and requires a communication service that must be reliable and have small latency. The target latency is in the order of 1 ms, more than one order of magnitude smaller than the latency of current 4G systems. In order to achieve such an ambitious target, the PHY latency of future 5G networks should not exceed 200-300 μs. Other applications, such as on-line gaming and car-to-car and car-to-infrastructure communications, although not directly related to the concept of the tactile Internet, also can take advantage of the low latency requirements [3].
- **Wireless Regional Area Networks (WRAN)**. It is expected that the generous throughput of 5G networks will also suit it to bringing internet broadband access to sparsely populated areas that are not yet covered by wired technologies such as ADSL and optical fiber. In this scenario network devices will have very low mobility, so Doppler effects will be negligible, and also latency will not be a key requirement. In order to be able to meet the throughput demands of bandwidth-hungry residential users, the use of so-called "white spaces" – in other words frequency bands licensed to other services but actually not used – seems unavoidable. It is thus anticipated that the available frequency bands will not be contiguous, and cognitive-like opportunistic spectrum access is a viable option. Millimeter wave frequencies (larger than 20 GHz) also will be used. The modulation format of future 5G systems should thus be able to efficiently exploit the available fragmented and heterogeneous spectrum.

Orthogonal frequency division multiplexing (OFDM) and orthogonal frequency division multiple access (OFDMA) are the modulation technique and the multiple access strategy adopted in long term evolution (LTE) 4G cellular network standards, respectively [4]. OFDM and OFDMA are based on a multicarrier approach and succeeded code division multiple access, as employed in 3G networks, and which was mostly based on a single-carrier approach. Among the chief advantages of OFDM and OFDMA are:

- the ease of implementation of both transmitter and receiver thanks to the use of fast Fourier transform (FFT) and inverse fast Fourier transform (IFFT) blocks
- the ability to counteract multi-path distortion
- the orthogonality of subcarriers, which eliminates intercell interference
- their easy coupling with adaptive modulation techniques
- the ease of integration with multi-antenna hardware, both at the transmitter and receiver.

Nonetheless, there are some key characteristics that make OFDM/OFDMA a less-than-perfect match for the above reference scenarios. First of all, OFDM is based on the use of rectangular pulses in the time domain, which leads to a slowly decaying behavior in the frequency domain; this makes OFDM unsuited for use in fragmented spectrum scenarios, where strict constraints on the out-of-band (OOB) levels are to be fulfilled. In 4G systems, OOB emissions are controlled by inserting null tones at the spectrum edges or, alternatively, by filtering the whole OFDM signal with a selective filter (this is usually known as filtered-OFDM). Both solutions unfortunately lead to a loss in spectral efficiency, since in the former case some of the available subcarriers are actually not modulated, while in the latter case we need a longer cyclic prefix to combat the time dispersion induced by the filtering operation. The need for a long cyclic prefix (CP) in heavy multipath environments is then another factor that degrades the system spectral efficiency. Likewise, the need for strict frequency and time synchronization among blocks and subcarriers in order to maintain orthogonality is a requirement that does not match well with the IoT scenario, wherein many devices have to access the channel with short data frames. Synchronization is also a key issue in the uplink of a cellular network wherein different mobile terminals transmit separately [5], and in the downlink, when base station coordination is used [6, 7]. Additionally, OFDM signals may exhibit large peak-to-average-power ratio (PAPR) values [8], and this has a clear impact on the system energy efficiency.

Based on the above considerations, a very active research track in the area of 5G systems has focused on the search for alternative modulation schemes capable of overcoming the disadvantages of OFDM/OFDMA [9],[2] and of supporting in an optimal way the emerging services and reference scenarios that we have discussed here. The main goal of this research activity is to look for modulation formats with low OOB emissions – so as to fully exploit the fragmented spectrum – and which do not not require a strict orthogonality among subcarriers, so as to simplify synchronization and access procedures.

This chapter provides a review of some of the best recently proposed alternatives to OFDM. Due to space constraints, it is not possible to go deep into details about each modulation scheme; nonetheless, we give mathematical models and block-schemes of the transmitter for all the alternatives considered. We also provide a comparative analysis of these modulations, highlighting their pros and cons, and discussing their ability to operate in the 5G reference scenarios discussed above.

The rest of this chapter is organized into the following three sections. Section 1.2 is devoted to all major alternative modulation formats beyond OFDM, including filter-bank multicarrier

[2] The issue of beyond-OFDM modulation has been also extensively addressed in EU-funded research projects such as 5GNOW [10] and METIS2020 [11].

(FBMC), generalized frequency division multiplexing (GFDM), bi-orthogonal frequency division multiplexing (BFDM), universal filtered multicarrier (UFMC) and time-frequency packing (TFP). In Section 1.3, we will deal with the waveform choice issue by providing some shaping pulses that can be considered as alternatives to the rectangular pulse adopted in OFDM. Section 1.4 is the final section and contains further discussion and provides concluding remarks.

1.1.1 The LTE Solution: OFDM and SC-FDMA

The current 4G standard, the LTE system, is based on the use of the OFDM modulation for the downlink and of the single-carrier frequency division multiple access (SC-FDMA) technique for the uplink [4]. OFDM is an orthogonal block transmission scheme which, in ideal conditions, is not affected by intercarrier interference and intersymbol interference (ISI). Figure 1.1 shows a block scheme for the OFDM modem. A block of K QAM symbols $(s(1), s(2), \ldots, s(K))$ is mapped onto the available K subcarriers and then IFFT is performed. After the IFFT, the CP, whose length must be larger than the channel impulse response duration, is included in the data block, which is then sent to a single-carrier modulator for transmission. After propagation through the channel, the CP is removed, and the block of K observables is passed through an FFT transformation. In ideal conditions, it can be shown that the mth data sample at the output of the FFT block can be written as

$$Z(m) = H(m)s(m) + W(m) \tag{1.1}$$

where $H(m)$ and $W(m)$ are the mth FFT coefficients of the channel impulse response and of the additive disturbance, respectively. Based on Eq. (1.1), the soft estimate of the symbol $s(m)$, to be sent to the data decoding block, is obtained through a simple one-tap equalization:

$$\hat{s}(m) = Z(m)/H(m) \tag{1.2}$$

We also note that, in order to highlight the use of the CP, the OFDM technique that we have just described is sometimes referred to as "CP-OFDM". Despite its simplicity and the aforementioned immunity to multipath distortion, OFDM has some key drawbacks and among these one of the most severe is the large PAPR, which requires amplifiers with an extended linearity range. While in the downlink we can usually afford to have expensive amplifiers at the

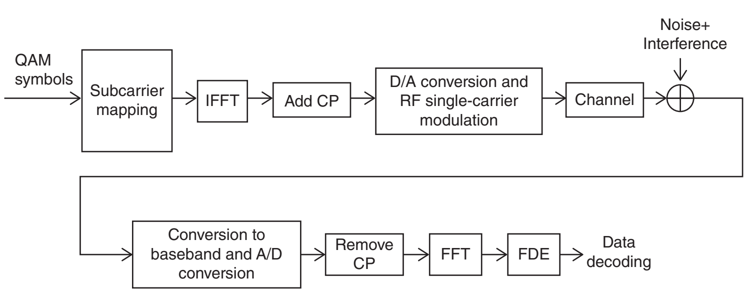

Figure 1.1 Principle of the OFDM modem

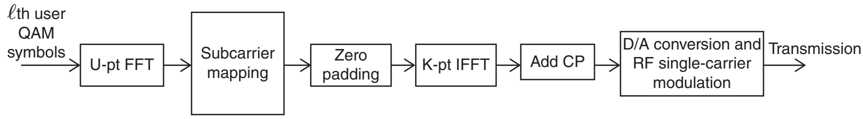

Figure 1.2 Block scheme of the SC-FDMA transmitter used in the uplink of LTE

transmitter (i.e. at the base station), this is not the case in the uplink, where the transmitter is a small mass-market mobile device. Accordingly, the modulation and multiple-access strategy used in the uplink of LTE is the so-called SC-FDMA strategy, a slightly different version of OFDM. Figure 1.2 depicts the typical SC-FDMA transmission scheme implemented in the generic ℓth user mobile device. Letting U denote the number of subcarriers (out of the available K) that have been assigned to the ℓth user in the current resource slot, a block of U QAM symbols is FFTed and mapped onto the assigned subcarriers. At the output of the "subcarrier mapping" block, the "zero padding" block forms a vector of K elements, containing zero values at the positions corresponding to the $K - U$ subcarriers that are not assigned to the ℓth user, and the ℓth user data at the remaining U positions. The K-dimensional block is passed through the IFFT block, then a CP is added and, after upconversion, signal transmission happens. Note that, according to the OFDMA principle, the active users must transmit synchronously so that the base station receiver is able to simultaneously collect the data from the users that are using the K available subcarriers. Due to the U-points FFT operation, the SC-FDMA strategy exhibits a PAPR smaller than that of pure OFDMA, since the transmitted signal is basically equivalent to an oversampled single-carrier signal.

1.2 New Modulation Formats: FBMC, GFDM, BFDM, UFMC and TFP

We now review some of the modulation schemes that are being considered for adoption in future 5G wireless networks.

1.2.1 Filter-bank Multicarrier

As is well-known, in the presence of multi-path channels, plain orthogonal multicarrier modulation formats are not able to maintain orthogonality due to ISI among consecutive multicarrier symbols. The traditional approach in OFDM to counter this issue is to introduce a CP longer than the time spread introduced by the channel. This enables the preservation of traditional transceiver implementations by IFTT and FFT operations, but introduces a time overhead in the communication, resulting into a loss of spectral efficiency.

The approach used by FBMC to overcome this issue is to keep the symbol duration unaltered, thereby avoiding the introduction of any time overhead, and to cope with the overlap among adjacent multicarrier symbols in the time domain by adding an additional filtering at the transmit and receive side, besides the IFFT/FFT blocks. This is done by filtering each output of the FFT by a frequency-shifted version of a lowpass filter $p(t)$, termed a "prototype" filter. This additional filtering, together with the IFFT/FFT operation, forms a synthesis-analysis filter-bank structure, where the prototype filter is designed to significantly suppress ISI.

To begin with, it is worthwhile to observe that the conventional OFDM scheme can also be regarded as an FBMC scheme, with a low-pass FIR prototype filter, with discrete-time impulse response given by

$$p(n) = \begin{cases} \frac{1}{N} & \forall\, n = 1, \ldots, N \\ 0 & \text{elsewhere} \end{cases} \tag{1.3}$$

To see this, let us observe that the input–output relation for the point of index $k = 0$ of an N-point DFT operating on the samples $\{x(n-i)\}_{i=1}^{N}$ can be expressed as:

$$y_0(n) = \frac{1}{N}\sum_{i=1}^{N} x(n-i) \tag{1.4}$$

which can be regarded as the input – output relation of the FIR filter with impulse response in Eq. (1.3). A similar relation can be obtained for the generic nth DFT coefficient, accounting for the frequency shift $e^{-j2\pi ni/N}$. As a consequence, we find that conventional OFDM schemes can be regarded as a particular FBMC scheme with rectangular pulses as prototype filters. However, such a choice of prototype filter does not protect against the ISI caused by multi-path channels. Instead, a prototype filter that guarantees significant ISI suppression is obtained by introducing additional coefficients between the FFT coefficients in the frequency domain. In particular, the number of introduced coefficients between two consecutive DFT coefficients is called the "overlapping factor" of the filter K, which is also equal to the ratio between the filter impulse response duration and the multicarrier symbol period T, thereby determining the number of multicarrier symbols which overlap in the time domain [12]. One prototype filter that is able to ensure a low ISI is that with impulse response:

$$p(t) = 1 + 2\sum_{k=1}^{K-1} H_k \cos\left(2\pi\frac{kt}{KT}\right) \tag{1.5}$$

where the coefficients H_k are given in Table 1.1, up to $K = 4$.

The samples of the frequency response of $p(t)$ are also reported in Figure 1.3.

From the above discussion, it would seem that a frequency spreading by a factor K is necessary to implement the FBMC scheme. Indeed, one possible implementation is based on a frequency spreading plus a KN-point IFFT at the transmitter, and on a KN-point FFT followed by a despreading at the receiver. This particular implementation has the advantage of requiring only minor modifications with respect to the traditional implementation of OFDM transmissions. However, increasing the FFT size by a factor K poses significant complexity issues. In order to reduce the computational complexity, an alternative implementation has been proposed. This is called polyphase network-FFT (PPN-FFT). PPN-FFT requires no frequency spreading, but at the expense of some additional processing. In the rest of this section this latter approach will be described.

Table 1.1 Frequency-domain prototype filter coefficients

K	H_0	H_1	H_2	H_3
2	1	$\sqrt{2}/2$	-	-
3	1	0.911438	0.411438	-
4	1	0.971960	$\sqrt{2}/2$	0.235147

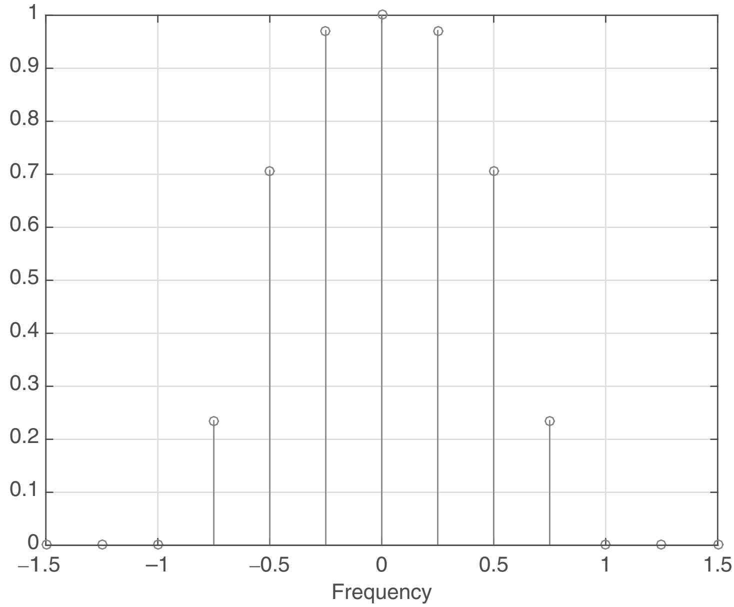

Figure 1.3 Frequency-domain samples of the prototype filter

Let us assume that the time-domain length of the prototype filter can be written as $L = KN$, and let us denote by $\{h_\ell\}_{\ell=1}^{L-1}$ the time-domain filter coefficients. Then, the frequency response of the prototype filter can be written as

$$P_0(f) = \sum_{\ell=0}^{L-1} h_\ell e^{-j2\pi\ell f} = \sum_{p=0}^{N-1} H_p(f) e^{-j2\pi p f} \tag{1.6}$$

where, for all $p = 0, \ldots, N-1$, we have defined the functions

$$H_p(f) = \sum_{k=0}^{K-1} h_{kN+p} e^{-j2\pi f k N} \tag{1.7}$$

We can see that Eq. (1.7) can be regarded as the frequency response of a phase shifter, which gives the name to this implementation of the FBMC modulation scheme. Next, we can obtain the frequency response of the nth filter of the bank by shifting Eq. (1.6) in the frequency domain by a factor n/N. This yields:

$$\begin{aligned} P_n(f) &= \sum_{p=0}^{N-1} H_p(f - n/N) e^{-j2\pi p(f-n/N)} \\ &= \sum_{p=0}^{N-1} \left(\sum_{k=0}^{K-1} h_{kN+p} e^{-j2\pi(f-n/N)kN} \right) e^{-j2\pi p(f-n/N)} \\ &= \sum_{p=0}^{N-1} H_p(f) e^{-j2\pi p f} e^{j2\pi p n/N} \end{aligned} \tag{1.8}$$

where we have exploited the fact that $e^{j2\pi kn} = 1$ for all $k = 0, \ldots, K-1$ and $n = 0, \ldots, N-1$. Then, considering the relations in Eq. (1.6) for all $n = 0, \ldots, N-1$, we can obtain the matrix equation:

$$\begin{pmatrix} P_0(f) \\ P_1(f) \\ \vdots \\ P_{N-1}(f) \end{pmatrix} = \begin{pmatrix} 1 & 1 & 1 & 1 \\ 1 & e^{j2\pi/N} & \cdots & e^{j2\pi(N-1)/N} \\ \vdots & \vdots & \vdots & \vdots \\ 1 & e^{j2\pi(N-1)/N} & \cdots & e^{j2\pi(N-1)^2/N} \end{pmatrix} \begin{pmatrix} H_0(f) \\ e^{-j2\pi f} H_1(f) \\ \vdots \\ e^{-j2\pi(N-1)f} H_{N-1}(f) \end{pmatrix} \tag{1.9}$$

Observing that the square matrix in Eq. (1.9) performs an IDFT operation, and recalling that the final output is obtained by summing the outputs of the individual filters of the bank, we determine that the transmitter of a PPN-FFT system can be implemented as shown in Figure 1.4. A similar scheme is used at the receiver, with the difference that the FFT operation is used in place of the IFFT, and that the frequency shifts are multiples of $-1/N$.

In conclusion, the PPN-FFT scheme can be implemented by adding the phase shifters $e^{-j2\pi pf} H_p(f)$ in series with the usual IFFT/FFT operation performed in conventional OFDM schemes. This entails a slight complexity increase with respect to OFDM, but still results in less complexity than applying a frequency spreading to implement the FBMC scheme.

1.2.2 Generalized Frequency Division Multiplexing

GFDM is a generalized multicarrier modulation that is particularly attractive in scenarios with fragmented spectrum [13, 1]. Indeed one of its main features is its low level of OOB emissions, which makes it well suited for transmission on non-contiguous frequency bands with strict spectral mask constraints. Thanks to the use of the CP, it retains OFDM advantages in

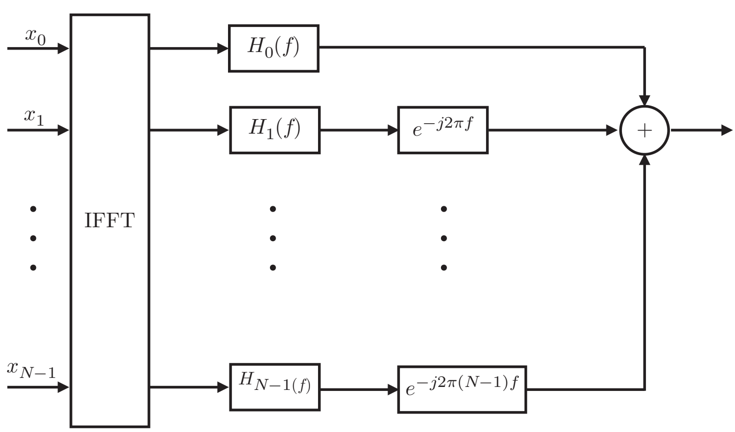

Figure 1.4 PPN-FFT implementation of the transmitter in the FBMC modulation scheme

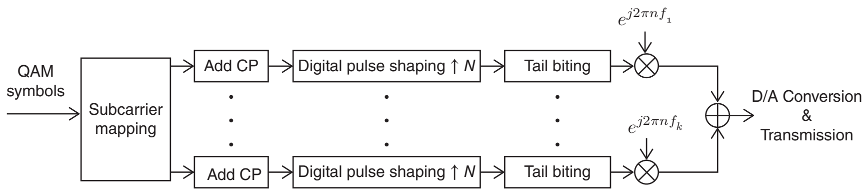

Figure 1.5 The GFDM transmitter

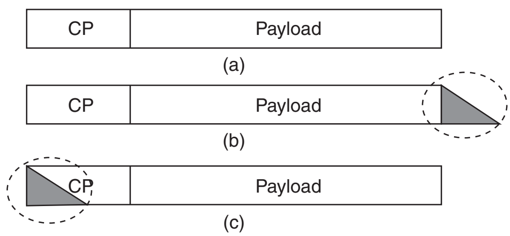

Figure 1.6 The tail-biting operation. (a) the CP is appended to the payload – its length must be set according to the duration of the channel impulse response and of the receive filter impulse response; (b) after passing through the transmit filter, the data packet is longer due to the convolution effect; (c) original length is restored by tail biting and adding the tail to the CP in order to emulate circular convolution

terms of robustness to multipath channels and ease of equalization, and may be efficiently implemented through signal processing in the digital domain. Inspecting Figure 1.5, wherein the block-scheme of a GFDM transmitter is presented, it is seen that GFDM is a pure multicarrier scheme that transmits parallel data streams on carrier frequencies $f_1, f_2, \ldots, f_K$, which are not required to be contiguous. A CP is used to combat time dispersion induced by all the filters, from the transmitter through channel to receiver. In contrast to legacy OFDM, where the CP length is simply required to be larger than the channel impulse response, in GFDM the CP should in principle have a length larger than the sum of the impulse responses of the transmit shaping filter, the channel, and the receive filter. The limitation of the OOB emissions is obtained through the use of pulse shapes; the lower the required OOB emissions, the longer the pulse length in the time domain. An efficient strategy for reducing the length of the CP and, equivalently, the loss in terms of spectral efficiency, is the tail-biting technique [13], the principle of which is shown in Figure 1.6. In this technique, the CP may be chosen to be as long as the sum between the impulse responses of the channel and that of the reception filter – in other words the transmit filter impulse response length is not taken into account – provided that, at the output of the transmit shaping filter, the additional samples that arise from the linear convolution are removed and added at the beginning of the data packet, so as to emulate circular convolution (see Figure 1.6 for an illustration of this operation). Note also that a similar procedure, not described here for the sake of brevity, can be used to reduce the CP length tied to the receive filter.

To provide a mathematical expression for the signal formed by the GFDM transmitter, we use the following notation:

- K denotes the number of available carrier frequencies; the baseband equivalent of the kth frequency band is centered on f_k;
- M denotes the number of QAM symbols forming the data block to be sent on each carrier;
- the M QAM symbols $s(0,k), s(1,k), \ldots, s(M-1,k)$ form the data block to be sent on the kth frequency band, while the $M + M_{CP}$ QAM symbols $\tilde{s}(0,k), \tilde{s}(1,k), \ldots, \tilde{s}(M + M_{CP} - 1, k)$ form the data block at the output of the CP block (see Figure 1.5);
- the transmit pulse is denoted $g_{tx}(n)$ and is a FIR filter of length QN, with N being the number of samples per data interval and Q being the number of signaling intervals that are spanned by the continuous-time version of the transmit pulse; note that the longer the value of Q, the larger the gain in terms of reduction of OOB emissions.

Based on the above notation, the signal at the input of the tail-biting block on the kth branch (carrier) of the transmitter in Fig 1.5 is expressed as

$$x_k(n) = \sum_{m=0}^{M+M_{CP}-1} \tilde{s}(m,k) g_{tx}(n - mM) \tag{1.10}$$

with $n = 0, \ldots, (M + M_{CP} + Q - 1)N - 1$. The subsequent tail-biting procedure reduces the length of this packet of $(Q-1)N$ samples.

One possible receiver architecture is shown in Figure 1.7. Thanks to the use of tail biting and the CP, all linear convolutions are turned into circular convolutions, and one-tap equalization in the frequency domain can be used to remove the ISI introduced by the channel and by the filtering operations. Indeed, after the CP prefix has been removed, we have, on the generic kth branch of the receiver, M data samples which are FFTed in order to obtain the frequency bins $Z(m,k)$:

$$Z(m,k) = S(m,k)H(m,k) + W(m,k) \tag{1.11}$$

where $S(m,k)$ is the mth FFT coefficient of the original QAM data symbols $s(0,k), \ldots, s(M-1,k)$, $W(m,k)$ is the mth FFT coefficient of the rx-filtered overall additive disturbance (i.e. AWGN noise plus adjacent channels interference), and, finally, $H(m,k)$ is the mth FFT coefficient of the impulse response of the composite channel, which is obtained as the convolution of the transmit filer, propagation channel and reception filter.

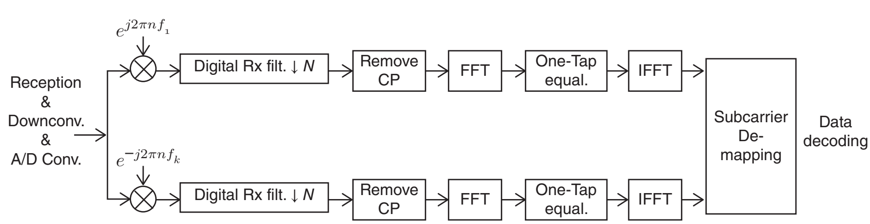

Figure 1.7 Diagram of a possible GFDM receiver

1.2.3 Bi-orthogonal Frequency Division Multiplexing

BFDM is a generalization of the classical CP-OFDM scheme and is able to provide lower intercarrier interference (ICI) and lower ISI. The basic idea is to introduce additional degrees of freedom into the system, which can be designed to obtain the said advantages.

Classical OFDM schemes are based on the orthogonality principle, according to which the prototype filter $g(t)$ should be orthogonal to a suitable time-frequency shifted version of itself, in other words:

$$\left\langle g(t), g(t-\ell T)e^{j2\pi nF(t-\ell T)} \right\rangle = 0, \quad \forall\, \ell, n \neq 0 \tag{1.12}$$

where T is the symbol interval and F is the frequency spacing among adjacent subcarriers. It is known that, due to channel distortions, the orthogonality of the transmissions might be lost unless a CP is used to introduce a guard-time among different symbols. However, this causes an extension of the time duration of the prototype filter, which is suboptimal in doubly dispersive channels because the time and frequency dispersions introduced by the channel are treated differently [14]. A way to overcome this issue is to observe that to obtain perfect demodulation (in the noiseless case) Condition (1.12) is only sufficient but not necessary. Specifically, Condition (1.12) implies that the same filter is used at the transmitter and receiver, but perfect demodulation (in the noiseless case) can also be obtained when the receiver employs a different receive filter, say $\gamma(t)$, provided the following bi-orthogonality condition is met:

$$\left\langle g(t), \gamma(t-\ell T)e^{j2\pi nF(t-\ell T)} \right\rangle = 0, \quad \forall\, \ell, n \neq 0 \tag{1.13}$$

The use of different transmit and receive pulses is precisely the additional degree of freedom enabled by the BFDM modulation scheme. The transmit and receive filters should be designed in order to fulfill Eq. (1.13), while at the same time ensuring low ICI and ISI. A necessary condition for Eq. (1.13) to hold is $TF \geq 1$ [15]. In practice, TF ranges between 1.03 and 1.25, which ensures a good trade-off between spectral efficiency and pulse localization [16, 17].

In doubly dispersive channels, the power of the ICI and ISI depends on the joint time-frequency concentration of the transmit and receive pulses. In more detail, a measure of the power of the ICI and ISI of BFDM is given by the cross-ambiguity function between the transmit and receive pulse, defined as

$$A_{\gamma,g}(\tau,\nu) = \int_t \gamma(t) g^*(t-\tau) e^{-j2\pi\nu t} dt \tag{1.14}$$

Therefore, the transmit pulse $g(t)$ and the receive pulse $\gamma(t)$ should be designed in order to achieve a suitable time-frequency localization. In particular, the following localization properties are desirable [16, 17].

Definition 1.1 *The pulses $g(t)$ and $\gamma(t)$ are said to be polynomially localized of degree $s \geq 0$ if there exists $T_0 > 0$ such that*

$$\int_\tau \int_\nu |A_{\gamma,g}(\tau,\nu)| \left(1 + \left|\frac{\tau}{T_0}\right| + |\nu T_0|\right)^s d\tau d\nu < \infty \tag{1.15}$$

A stronger localization property is the sub-exponential localization.

Definition 1.2 *The pulses $g(t)$ and $\gamma(t)$ are said to be sub-exponentially localized if there exist $T_0 > 0$, $b > 0$, and $\beta \in (0,1)$ such that*

$$\int_\tau \int_\nu |A_{\gamma,g}(\tau,\nu)| e^{b(|\tau/T_0|+|\nu T_0|)^\beta} d\tau d\nu < \infty \tag{1.16}$$

In practice spline-type pulses are used to obtain a polynomial localization whereas Gaussian pulses enable an exponential localization.

1.2.4 Universal Filtered Multicarrier

Universal Filtered Multicarrier (UFMC) is a multicarrier modulation format that has been proposed by the EU-funded research project 5GNOW [3, 18, 19, 20, 21]. UFMC admits as particular cases the filtered-OFDM and the FBMC modulations. Indeed, while in the former case the whole set of subcarriers is filtered to limit sidelobe effects, and while in FBMC modulations filtering is applied separately to each subcarrier, in UFMC subcarriers are filtered in groups. Denoting again by K the overall number of subcarriers, let us assume that these K subcarriers are divided in B separate groups; although groups are allowed to be composed of different numbers of subcarriers, for the sake of simplicity we assume here that each group is composed of P subcarriers, so that $K = BP$.

Denote now by $\mathbf{s}_1, \mathbf{s}_2, \ldots, \mathbf{s}_B$ the P-dimensional vectors containing the QAM data symbols to be transmitted, and by $\mathbf{V}$ the $(K \times K)$ IFFT matrix; we partition this matrix using the B submatrices $\mathbf{V}_1, \ldots, \mathbf{V}_B$, each of dimension $(K \times P)$:

$$\mathbf{V} = [\mathbf{V}_1 \ \mathbf{V}_2 \ \ldots \ \mathbf{V}_B \ ] \tag{1.17}$$

Equipped with this notation, we can now illustrate the UFMC transmitter operation (see Figure 1.8). The B data vectors $\mathbf{s}_1, \ldots, \mathbf{s}_B$ are processed with the IDFT submatrices $\mathbf{V}_1, \ldots, \mathbf{V}_B$, respectively. Then, they are passed through a pulse shape of length N_g, aimed at attenuating sidelobe levels in the frequency domain, and summed together (see Figure 1.8). In principle, we may use different filters for each branch. Denoting by $\mathbf{F}_i$ the $((K + N_g - 1) \times K)$ Toeplitz matrix describing the convolution operation with the shaping filter, the discrete-time signal to be converted to the analog domain and transmitted at RF is expressed as

$$\mathbf{x} = \sum_{i=1}^{B} \mathbf{F}_i \mathbf{V}_i \mathbf{s}_i \tag{1.18}$$

At the receiver side, denoting by $\mathbf{H}$ the Toeplitz matrix, of dimension $(K + N_g + N_h - 2) \times ((K + N_g - 1))$, where N_h is the length of the propagation channel, and describing linear convolution with the channel impulse response, the discrete-time baseband equivalent of the received signal is given by the following $(K + N_g + N_h - 2)$-dimensional vector:

$$\mathbf{y} = \mathbf{H} \left(\sum_{i=1}^{B} \mathbf{F}_i \mathbf{V}_i \mathbf{s}_i \right) + \mathbf{w} \tag{1.19}$$

with $\mathbf{w}$ being the additive disturbance, made of noise plus possible co-channel interference. It can be seen that Eq. (1.19) describes a classical linear model, and a plethora of well-known

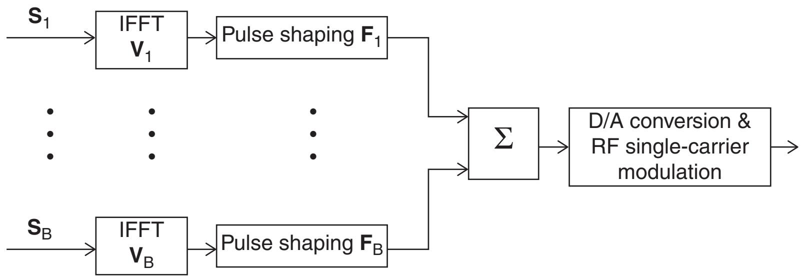

Figure 1.8 The UFMC transmitter

signal processing techniques – matched filtering, linear minimum mean square error estimation, zero-forcing detection and so on – can be used to recover the QAM symbols. Classical FFT-based processing with attendant one-tap equalization in the frequency domain is also possible.

1.2.5 Time-frequency Packing

In traditional digital communications, orthogonal signaling has been often adopted to ensure the absence of ISI and ICI. However, when finite-order constellations are used, it is possible to increase the spectral efficiency of communication systems by giving up the orthogonality condition and by introducing a controlled interference into the signal. This idea was first introduced by Mazo for single-carrier transmissions with the name of faster-than-Nyquist (FTN) signaling [22]. FTN signaling is a linear modulation technique that reduces the time spacing between two adjacent pulses (the symbol time) to well below that ensuring the Nyquist condition, thus introducing controlled ISI [22, 23, 24]. If the receiver can cope with the ISI, the efficiency of the communication system is increased. In the original papers on FTN signaling [22, 23, 24], this optimal time spacing is obtained as the smallest value giving no reduction of the minimum Euclidean distance with respect to the Nyquist case. This ensures that, asymptotically, the ISI-free bit-error rate (BER) performance is reached when optimal detectors are used. More recently, this concept has been extended to multicarrier transmissions by Rusek and Anderson [24]. In this case, intentional ICI is also introduced by reducing the frequency separation among carriers.

A multicarrier FTN signal can be expressed as

$$x(t) = \sqrt{E_{\mathrm{s}}} \sum_{n} \sum_{\ell} x_n^{(\ell)} p(t - n\delta_{\mathrm{t}} T) e^{j2\pi \ell \delta_{\mathrm{f}} F t} \tag{1.20}$$

where E_{s} is the average energy per symbol, $x_n^{(\ell)}$ is the M-ary symbol transmitted during the nth signaling interval over the ℓth carrier, $p(t)$ is the base pulse, usually a pulse with root raised cosine (RRC) spectrum with roll-off α, and T and F are the symbol time and frequency spacing that ensure orthogonality in the time and frequency domains, respectively.[3] The coefficients $\delta_{\mathrm{t}} \leq 1$ and $\delta_{\mathrm{f}} \leq 1$ are the compression factors for the symbol interval and frequency spacing, respectively. While setting them to 1 results in an orthogonal transmission, they can

[3] As far as F is concerned, its minimum value is $F = \frac{1+\alpha}{T}$.

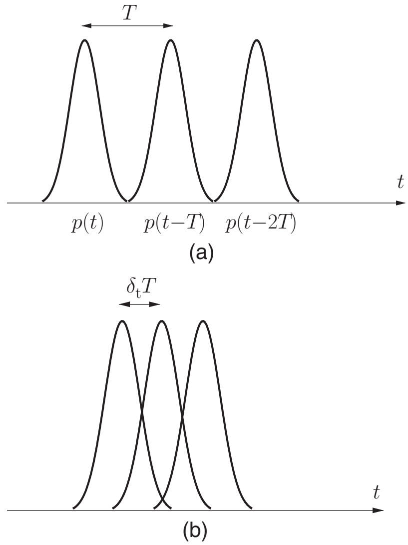

Figure 1.9 Schematic view of (a) orthogonal and (b) FTN signaling in the time domain

be reduced to a given extent without reducing the minimum Euclidean distance. The effects of the application of FTN in the time domain are schematically represented in Figure 1.9, which shows the transmission of a generic pulse $p(t)$ with orthogonal signaling (Figure 1.9(a)) and adopting a coefficient $\delta_{\mathrm{t}} < 1$ (Figure 1.9(b)). We can see how interference from adjacent pulses arises in the latter case.

Some scepticism can be raised against this technique. From a practical point of view, FTN may require an optimal detector, the complexity of which easily becomes unmanageable. No hints are provided in the original papers as to how to perform the optimization in the more practical scenario where a reduced-complexity receiver is employed. From a theoretical point of view, although this technique has been proposed to increase the spectral efficiency of a communication system, the uncoded BER is used as figure of merit in place of the spectral efficiency itself.

Before discussing ways to solve these problems, we need to introduce a few definitions. Let us consider the multicarrier transmission in Eq. (1.20), where $\delta_f F$ is the frequency separation between two adjacent carriers and $\delta_t T$ is the symbol time. We will collect in a vector $\mathbf{x}^{(\ell)} = \{x_k^{(\ell)}\}$ the input symbols transmitted over the ℓth carrier. At the receiver side, a discrete-time set of sufficient statistics is extracted using a bank of matched filters and we denote by $\mathbf{y}^{(\ell)} = \{y_k^{(\ell)}\}$ the samples at the output of the matched filter for the ℓth carrier.

Depending on the allowed complexity at the receiver, different strategies can be adopted for detection. For example, the receiver can neglect both ICI and ISI and adopt a symbol-by-symbol detector. In other words, instead of the optimal receiver for the actual channel, we could adopt the optimal receiver for a simplified auxiliary channel, for which the combined effect of ISI and ICI is modeled as a zero-mean Gaussian process independent of the additive thermal noise. Note that the interference is truly Gaussian distributed only if the transmitted symbols are Gaussian distributed as well and this is not the case in practice. Especially when the interference set is small – for example when δ_t and δ_f are close to one – the actual interference distribution may substantially differ from a Gaussian distribution. However, the accuracy of this approximation is not of concern here: assuming Gaussian-distributed interference is required for the auxiliary channel model anyway, to ensure that a symbol-by-symbol receiver is optimal. It is like saying that the Gaussian assumption is a *consequence* of the choice of the symbol-by-symbol receiver. Once the simplified receiver has been selected – suboptimal for the channel at hand but optimal for the considered auxiliary channel – it is possible to compute a lower bound on the information rate for that channel using the technique of Arnold *et al*. [25]. The information rate, also called constrained capacity, is the mutual information when the input symbols are constrained to belong to our finite constellation $\mathcal{X}$. According to mismatched detection [26], this lower bound is *achievable* by that particular suboptimal detector. The achievable spectral efficiency (ASE) is defined as the ratio between the achievable lower bound on the information rate and the product $\delta_\mathrm{f} F \delta_\mathrm{t} T$

$$\mathrm{ASE} = \frac{I(\mathbf{x}^{(\ell)}; \mathbf{y}^{(\ell)})}{\delta_\mathrm{f} F \delta_\mathrm{t} T}$$

where $\delta_\mathrm{f} F$ is a measure of the bandwidth of the given subcarrier.

The most recent extension of the FTN principle is thus time-frequency packing [27], in which it is proposed to optimize δ_f and δ_t in order to maximize the ASE. The idea is very simple: by reducing δ_f and δ_t the achievable information rate $I(\mathbf{x}^{(\ell)}; \mathbf{y}^{(\ell)})$ will certainly degrade due to the increased interference. However, the spectral efficiency – in other words $I(\mathbf{x}^{(\ell)}; \mathbf{y}^{(\ell)})/\delta_\mathrm{f} F \delta_\mathrm{t} T$ – can be improved. Hence, the main quantity of interest is not the uncoded BER performance.[4] We may accept a degradation of the information rate provided the spectral efficiency is increased. In other words, instead of keeping the same code, an improvement can be obtained by using a code with a lower rate. Improving the spectral efficiency without increasing the constellation size is convenient since low-order constellations are more robust to impairments such as phase noise and nonlinearities.

In Ref. [27], the main concepts are elucidated with reference to a symbol-by-symbol detector and the additive white Gaussian noise (AWGN) channel, working on the samples at the matched filters output. More sophisticated receiver architectures are considered in Ref. [28], still with reference to the AWGN channel. In general, there are several receiver architectures that have been considered for the detection of TFP signals, that include equalization [29] and filtering, followed by a maximum a posteriori (MAP) symbol detector based, for example, on a BCJR algorithm [30]. One of such advanced filtering techniques is the so-called 'channel shortening' [31], aimed at designing the interference at the MAP detector to properly fit the desired complexity of the detection stage. Further gains can be obtained by using algorithms that detect more than one carrier at a time. In general, the larger the receiver complexity, the higher the gains that this technique can achieve. Its effectiveness has been demonstrated in several scenarios on wireless and optical channels [9, 28, 32, 33], and it appears to be suited for 5G systems as well.

[4] Since there is no need to keep the same Euclidean distance as the Nyquist case, there is no need to employ a base pulse satisfying the Nyquist condition. Thus TFP can be adopted for *any* base pulse.

1.2.6 Single-carrier Schemes

All of the modulation formats considered so far employ multicarrier transmissions. However, while multicarrier formats are compatible with most of the candidate technologies for 5G networks, they might not be the best choice if millimeter waves (mmWaves) are employed.

The use of mmWaves has been proposed as a strong candidate for achieving the spectral efficiency growth required by 5G networks, resorting to the use of the currently unused frequency bands in the range between 20 GHz and 90 GHz. In particular, the E-band, between 70 GHz and 80 GHz, provides 10 GHz of free spectrum, which could be exploited to operate 5G networks. Up until now, the use of mmWaves for cellular communications has been neglected due to the higher atmospheric attenuation that they suffer compared to other frequency bands. However, while this is true for propagation in the macro-cell environments that are typical of past cellular generations, recent measurements suggest that mmWave attenuation is only slightly worse than in other bands, as far as propagation in dense urban environments is concerned [34]. Therefore, mmWaves have recently been reconsidered as a viable technology for cellular communications.

One of the main advantages of multicarrier schemes is their ability to multiplex users in the frequency domain. However, this advantage comes with several disadvantages too. Indeed, this chapter has been concerned with the analysis of possible alternatives to the conventional OFDM scheme, which cope with its shortcomings, but without renouncing the possibility of having a frequency-domain multiplex. However, if mmWaves are used, this feature might not be so crucial, for several reasons.

- As already mentioned, the propagation attenuation of mmWaves make them a viable technology only for small-cell, dense networks, where few users will be associated to any given base station.
- The higher bandwidth would cause low OFDM symbol duration, making it possible to multiplex users in the time domain as efficiently as in the frequency domain.
- mmWaves will be operated together with massive antenna arrays to overcome propagation attenuation. This makes digital beamforming unfeasible, since the energy required for digital-to-analog and analog-to-digital conversion would be huge. Thus, each user will have an own radio-frequency beamforming, which requires users to be separated in time rather than in frequency.

In light of these considerations, one possibility for mmWaves is to dispense with multicarrier transmissions, eliminating its drawbacks, and resorting instead to single-carrier (SC) modulation formats. In Ghosh *et al*. [35], the null cyclic prefix single carrier (NCP-SC) scheme has been proposed for mmWaves. The concept is to transmit a single-carrier signal in which the usual cyclic prefix used by OFDM is replaced by nulls appended at the end of each transmit symbol. The block scheme is shown in Figure 1.10.

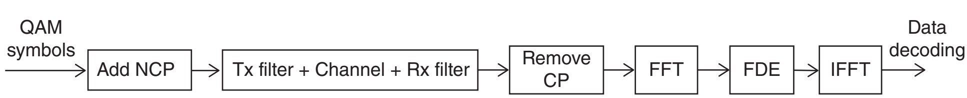

Figure 1.10 Principle of NCP-SC transceiver architecture

The NCP-SC scheme has several advantages over OFDM. In particular:

- The null cyclic prefix is part of the transmit symbol and is fed to the FFT together with the other data samples. This makes it possible to adapt the length of the prefix of each user, without disrupting the frame timing, because the length of each user's transmit symbol is always kept constant to N.
- The NCP-SC has a much lower PAPR and much lower OOB emissions than OFDM. This reduces interference and eases the design and operation of power amplifiers.
- The presence of time intervals in which no useful data are present makes it easier to estimate the interference-plus-noise power at the receiver.

Before concluding this section, it should also be observed that NCP-SC has some drawbacks compared to OFDM too. In particular, it requires a higher computational complexity. As we can see from the NCP-SC scheme in Figure 1.10, both an FFT and IFFT operations are required at the receiver. OFDM, on the other hand, only requires one FFT at the receiver. The resulting complexity increase might become significant, especially for increasing sizes of the FFT.

1.3 Waveform Choice

In this section, we describe some shaping pulses that can be considered as alternatives to the rectangular pulse adopted in OFDM. In practice, we are interested in pulses that achieve a good compromise between their sidelobe levels in the frequency domain, and their extension in the time-domain. The design of discrete-time windows with the discussed properties is a classical topic that arises in many areas of signal processing, such as FFT-based spectrum analysis and the synthesis of finite-impulse-response filters with the window method. Several pulse shapes are thus available in the open literature (see, for example, Proakis and Demetris [36] and Sahin *et al*. [37]). In what follows, we just give three possible examples, namely the evergreen RRC, the pulse proposed in the PHYDYAS research project for use with FBMC [38], and finally the Dolph–Chebyshev (DC) pulse, whose use has been recommended for the UFMC modulation.

- **RRC pulses** are widely used in telecommunication systems to minimize ISI at the receiver. The impulse response of an RRC pulse is

$$p(t) = \begin{cases} \frac{1}{\sqrt{T}}\left(1-\alpha+4\frac{\alpha}{\pi}\right) & t=0 \\ \frac{\alpha}{\sqrt{2T}}\left[\left(1+\frac{2}{\pi}\right)\sin\left(\frac{\pi}{4\alpha}\right)+\left(1-\frac{2}{\pi}\right)\cos\left(\frac{\pi}{4\alpha}\right)\right] & t=\pm\frac{T}{4\alpha} \\ \frac{1}{\sqrt{T}}\frac{\sin\left(\pi\frac{t}{T}(1-\alpha)\right)+4\alpha\frac{t}{T}\cos\left(\pi\frac{t}{T}(1+\alpha)\right)}{\pi\frac{t}{T}\left[1-\left(4\alpha\frac{t}{T}\right)^2\right]} & \text{otherwise} \end{cases}$$

  where T is the symbol interval and α is the roll-off factor, which measures the excess bandwidth of the pulse in the frequency domain.
- **The PHYDYAS pulse** is a discrete-time pulse specifically designed for FBMC systems. Let M be the number of subcarriers. Then the impulse response is

$$p(n) = P_0 + 2\sum_{k=1}^{K-1}(-1)^k P_k \cos\left(\frac{2\pi k}{KM}(n+1)\right)$$

for $n = 0, 1, \ldots, KM - 2$ and $K = 4$, where the coefficients $P_k, k = 0, \ldots, K-1$ have been selected using the frequency sampling technique [38], and assume the following values:

$$P_0 = 1$$
$$P_1 = 0.97195983$$
$$P_2 = 1/\sqrt{2}$$
$$P_3 = \sqrt{1 - P_1}$$

- **The DC pulse** [39] is significant because, in the frequency domain, it minimizes the main lobe width for a given sidelobe attenuation. Its discrete-time impulse response is [40]:

$$p(n) = \frac{1}{N}\left[10^{-\frac{A}{20}} + 2\sum_{k=1}^{(N-1)/2} T_{N-1}\left(x_0 \cos\left(\frac{k\pi}{N}\right)\right)\cos\left(\frac{2\pi nk}{N}\right)\right]$$

for $n = 0, \pm 1, \ldots, \pm\frac{N-1}{2}$, where N is the number of coefficients, A is the attenuation of side lobes in dB,

$$x_0 = \cosh\left(\frac{1}{N-1}\cosh^{-1}\left(10^{-\frac{A}{20}}\right)\right)$$

and

$$T_n(x) = \begin{cases} \cos(n\cos^{-1}(x)) & |x| \leq 1 \\ \cosh(n\cosh^{-1}(x)) & |x| > 1 \end{cases}$$

is the Chebyshev polynomial of the first kind [41].

In Figure 1.11, we report the spectra of the pulses we have just described. All spectra were computed by performing a 1024 points FFT of pulses of 160 samples in the time domain. The figure compares the rectangular pulse, typical of OFDM, with an RRC pulse having roll-off $\alpha = 0.1$, the PHYDYAS pulse with $M = 1$, and the DC pulse with attenuation $A = -50$ dB. The figure clearly shows that the rectangular pulse is the one with the worst spectral characteristics; on the other hand, the PHYDYAS pulse is the one with the smallest sidelobe levels, while the DC pulse is the one with the smallest width of the main lobe.

1.4 Discussion and Concluding Remarks

This chapter has been devoted to the illustration of some of the most promising modulation schemes for use in forthcoming 5G cellular networks. While legacy OFDM is a robust and mature technology used in several communication systems – indeed, OFDM modulation is the core PHY technology of 4G systems, and is also employed in other systems such as digital audio broadcasting and terrestrial digital video broadcasting – the very stringent requirements of future networks, along with the heterogeneous scenarios that they will have to operate in, has pushed researchers to look for other solutions. One conclusion that can certainly be drawn is that what is the "best" modulation is a question that cannot be easily answered, and indeed

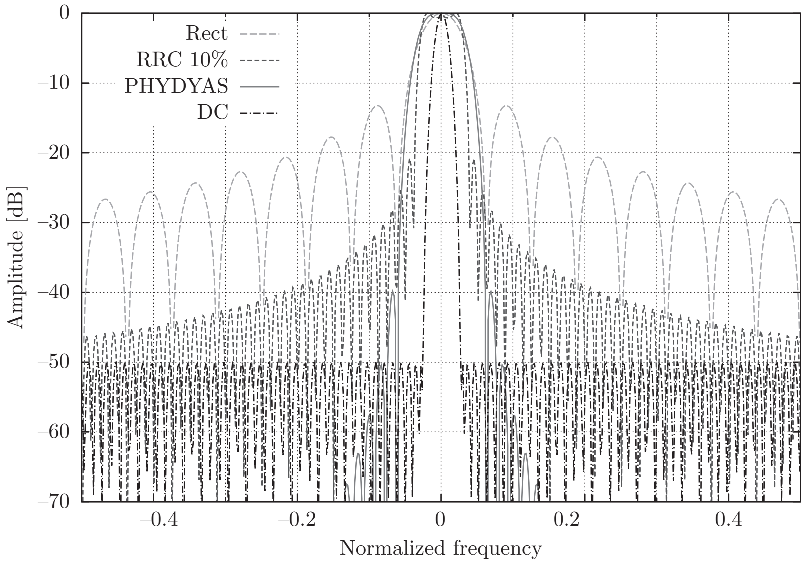

Figure 1.11 Comparison of pulse shapes in the frequency domain

the right answer might be "it depends", in the sense that there is no modulation that performs the best in all possible operating conditions. As an instance, UFMC, by virtue of its low side-lobe levels, is a modulation scheme that has been designed to perform well in scenarios where asynchronous transmissions and carrier frequency offsets may lead to ICI, although this property is retained by FBMC too. Due to its long shaping filters, FBMC unfortunately has a low efficiency in situations where small data packets are to be transmitted, a scenario typical of the IoT. Both UFMC and FBMC do not require the use of a CP, and this is a clear advantage with respect to filtered-OFDM, for instance. On the other hand, when dealing with access to fragmented spectrum, GFDM exhibits great flexibility, since frequency bands can be added and removed in a communication link quite easily and in a flexible way. The latency requirement also plays a key role and in this aspect FBMC again appears a weak choice since the long impulse response of its shaping filters prohibits its use in situations of sporadic traffic and low latency. Considering the issue of pure throughput maximization, it is evident that TFP appears to be the best choice, even though receiver complexity must be carefully taken into account, which makes this modulation clearly unsuited for IoT applications. In a WRAN scenario, on the other hand, in which a vast number of receivers are installed indoors and plugged into the electrical grid, high-complexity receiver are affordable and TFP might be a good option.

Ultimately, the solution to the problem of choosing a new modulation scheme will reside in the so-called software-defined-networking paradigm [42]. Indeed, the trend that we are witnessing in recent years is the increased role of software implementations with respect to hardware implementation of communication services. 5G networks will see a lot of functionality implemented via software as well. In addition, PHY-layer functions will be partly virtualized and implemented in a data-center. A virtualized PHY service will permit tuning of the modulation parameters to the scenario at hand; the modulation scheme itself might be changed according to the operating scenario. In this framework, one might think of a software-defined adaptive PHY, which would certainly be able to cope with the stringent levels of flexibility, scalability, performance and efficiency that 5G networks will require.

References

[1] Michailow, N., Matthé, M., Gaspar, I.S., Caldevilla, A.N., Mendes, L.L., Festag, A., and Fettweis, G. (2014) Generalized frequency division multiplexing for 5th generation cellular networks. *IEEE Trans. Commun.*, **62** (9), 3045–3061.

[2] Fettweis, G. (2014) The tactile internet: applications and challenges. *IEEE Veh. Tech. Mag.*, **9** (1), 64–70.

[3] Schaich, F., Wild, T., and Chen, Y. (2014) Waveform contenders for 5G – suitability for short packet and low latency transmissions, in *79th IEEE Vehic. Tech. Conf. 2014*, IEEE, pp. 1–5.

[4] Ghosh, A., Zhang, J., Andrews, J.G., and Muhamed, R. (2010) *Fundamentals of LTE*, Pearson Education.

[5] Morelli, M. (2004) Timing and frequency synchronization for the uplink of an OFDMA system. *IEEE Trans. Commun.*, **52** (2), 296–306.

[6] Hwang, T., Yang, C., Wu, G., Li, S., and Ye Li, G. (2009) OFDM and its wireless applications: a survey. *IEEE Trans. Veh. Tech.*, **58** (4), 1673–1694.

[7] Irmer, R., Droste, H., Marsch, P., Grieger, M., Fettweis, G., Brueck, S., Mayer, H.P., Thiele, L., and Jungnickel, V. (2011) Coordinated multipoint: Concepts, performance, and field trial results. *IEEE Commun. Mag.*, **49** (2), 102–111.

[8] Ochiai, H. and Imai, H. (2001) On the distribution of the peak-to-average power ratio in OFDM signals. *IEEE Trans. Commun.*, **49** (2), 282–289.

[9] Banelli, P., Buzzi, S., Colavolpe, G., Modenini, A., Rusek, F., and Ugolini, A. (2014) Modulation formats and waveforms for 5G networks: Who will be the heir of OFDM? *IEEE Signal Processing Mag.*, **31** (6), 80–93.

[10] 5GNow website, http://5gnow.eu.

[11] Metis Project website, http://www.metis2020.com.

[12] Bellanger, M. (2010) FBMC physical layer: a primer, *Tech. Rep*., PHYDYAS.

[13] Fettweis, G., Krondorf, M., and Bittner, S. (2009) GFDM - generalized frequency division multiplexing, in *Proc. Vehicular Tech. Conf.*, Barcelona, Spain, pp. 1–4.

[14] Kozek, W. and Molisch, A.F. (1998) Nonorthogonal pulseshapes for multicarrier communications in doubly dispersive channels. *IEEE J. Select. Areas Commun.*, **16** (8), 1579–1589.

[15] Gröchenig, K. (2001) *Foundations of Time-Frequency Analysis*, Birkhäuser.

[16] Matz, G. and Hlawatsch, F. (eds) (2011) *Fundamentals of Time-varying Communication Channels*, Academic Press.

[17] Matz, G., Bolcskei, H., and Hlawatsch, F. (2013) Time-frequency foundations of communications: concepts and tools. *IEEE Signal Processing Mag.*, **30** (6), 87–96.

[18] Wunder, G., Jung, P., Kasparick, M., Wild, T., Schaich, F., Chen, Y., Brink, S., Gaspar, I., Michailow, N., Festag, A. *et al*. (2014) 5GNOW: non-orthogonal, asynchronous waveforms for future mobile applications. *IEEE Commun. Mag.*, **52** (2), 97–105.

[19] Wunder, G., Kasparick, M., Brink, S., Schaich, F., Wild, T., Gaspar, I., Ohlmer, E., Krone, S., Michailow, N., Navarro, A. *et al*. (2013) 5GNOW: Challenging the LTE design paradigms of orthogonality and synchronicity, in *Proc. Vehicular Tech. Conf.*, Dresden, Germany.

[20] Vakilian, V., Wild, T., Schaich, F., Ten Brink, S., and Frigon, J.F. (2013) Universal-filtered multi-carrier technique for wireless systems beyond LTE, in *Globecom Workshops*, IEEE, pp. 223–228.

[21] Schaich, F. and Wild, T. (2014) Waveform contenders for 5G – OFDM vs. FBMC vs. UFMC, in *6th Int. Symp. Commun. Cont. Sig. Proc. (ISCCSP), 2014*, IEEE, pp. 457–460.

[22] Mazo, J.E. (1975) Faster-than-Nyquist signaling. *Bell System Tech. J.*, **54**, 1450–1462.

[23] Liveris, A. and Georghiades, C.N. (2003) Exploiting faster-than-Nyquist signaling. *IEEE Trans. Commun.*, **47**, 1502–1511.

[24] Rusek, F. and Anderson, J.B. (2005) The two dimensional Mazo limit, in *Proc. IEEE Int. Sympos. Info. Th.*, Adelaide, Australia, pp. 970–974.

[25] Arnold, D.M., Loeliger, H.A., Vontobel, P.O., Kavčić, A., and Zeng, W. (2006) Simulation-based computation of information rates for channels with memory. *IEEE Trans. Inform. Theory*, **52** (8), 3498–3508.

[26] Merhav, N., Kaplan, G., Lapidoth, A., and Shamai, S. (1994) On information rates for mismatched decoders. *IEEE Trans. Inform. Theory*, **40** (6), 1953–1967.

[27] Barbieri, A., Fertonani, D., and Colavolpe, G. (2009) Time-frequency packing for linear modulations: Spectral efficiency and practical detection schemes. *IEEE Trans. Commun.*, **57**, 2951–2959.

[28] Modenini, A., Colavolpe, G., and Alagha, N. (2012) How to significantly improve the spectral efficiency of linear modulations through time-frequency packing and advanced processing, in *Proc. IEEE Intern. Conf. Commun.*, Ottawa, Canada, pp. 3299–3304.

[29] Isam, S., Kanaras, I., and Darwazeh, I. (2011) A truncated SVD approach for fixed complexity spectrally efficient FDM receivers, in *Proc. IEEE Wireless Commun. and Network. Conf.*, Cancun, Mexico, pp. 1584–1589.

[30] Bahl, L.R., Cocke, J., Jelinek, F., and Raviv, J. (1974) Optimal decoding of linear codes for minimizing symbol error rate. *IEEE Trans. Inform. Theory*, **20**, 284–287.

[31] Rusek, F. and Prlja, A. (2012) Optimal channel shortening for MIMO and ISI channels. *IEEE Trans. Wireless Commun.*, **11** (2), 810–818.

[32] Piemontese, A., Modenini, A., Colavolpe, G., and Alagha, N. (2013) Improving the spectral efficiency of nonlinear satellite systems through time-frequency packing and advanced processing. *IEEE Trans. Commun.*, **61** (8), 3404–3412.

[33] Colavolpe, G. and Foggi, T. (2014) Time-frequency packing for high capacity coherent optical links. *IEEE Trans. Commun.*, **62**, 2986–2995.

[34] Ghosh, A., Thomas, T.A., Cudak, M., Ratasuk, R., Moorut, P., Vook, F.W., Rappaport, T., G. R, MacCartney, J., Sun, $\mathcal{S}$., and Nie, S. (2014) Millimeter wave enhanced local area systems: A high data rate approach for future wireless networks. *IEEE J. Select. Areas Commun.*, **32** (6), 1152–1163.

[35] Cudak, M. *et al*. (2013) Moving towards mmwave-based beyond-4G (b-4G) technology, in *Proc. IEEE 77th Vehic. Tech. Conf. Spring*.

[36] Proakis John, G. and Manolakis Dimitris, G. (1996) *Digital Signal Processing. Principles, Algorithms, and Applications*, Prentice Hall.

[37] Sahin, A., Guvenc, I., and Arslan, H. (2012) A survey on multicarrier communications: Prototype filters, lattice structures, and implementation aspects. *IEEE Commun. Surveys & Tut.*, **16** (3), 1312–1338.

[38] Viholainen, A., Bellanger, M., and Huchard, M. (2008) Prototype filter and structure optimization, *Tech. Rep.*, PHYDYAS.

[39] Dolph, C. (1946) A current distribution for broadside arrays which optimizes the relationship between beam width and side-lobe level. *Proc. IRE*, **34** (6), 335–348.

[40] Antoniou, A. (2000) *Digital Filters: Analysis, Design and Applications*, McGraw-Hill.

[41] Abramowitz, M. and Stegun, I.A. (eds) (1972) *Handbook of Mathematical Functions*, Dover.

[42] Rost, P., Bernardos, C., Domenico, A., Girolamo, M., Lalam, M., Maeder, A., Sabella, D. *et al*. (2014) Cloud technologies for flexible 5G radio access networks. *IEEE Commun. Mag.*, **52** (5), 68–76.